Continuous particle separation in a serpentine microchannel via negative and positive dielectrophoretic focusing

2010 J. Micromech. Microeng. 20 065011

(http://iopscience.iop.org/0960-1317/20/6/065011)

J. Micromech. Microeng. **20** (2010) 065011 (6pp) doi:10.1088/0960-1317/20/6/065011

Continuous particle separation in a serpentine microchannel via negative and positive dielectrophoretic focusing

Christopher Church, Junjie Zhu, Juan Nieto, Gyunay Keten, Erl Ibarra and Xiangchun Xuan[1]

Department of Mechanical Engineering, Clemson University, Clemson, SC 29634-0921, USA

E-mail: xcxuan@clemson.edu

Received 8 January 2010, in final form 11 March 2010
Published 11 May 2010
Online at stacks.iop.org/JMM/20/065011

Abstract
Dielectrophoresis (DEP) has been widely used to focus and separate cells and particles in microfluidic devices. This work first demonstrates negative and positive dielectrophoretic focusing of particles in a serpentine microchannel by changing only the electric conductivity of the suspending fluid. Due to the channel turn-induced dielectrophoretic force, particles are focused to either the centerline or the sidewalls of the channel when their electric conductivity is lower (i.e. negative DEP) or higher (i.e. positive DEP) than that of the fluid. These distinctive dielectrophoretic focusing phenomena in a serpentine microchannel are then combined to implement a continuous separation between particles of different sizes and electric conductivities. Such separation eliminates the fabrication of in-channel microelectrodes or micro-insulators that are typically required in DEP-based separation techniques. A numerical model is also developed to predict the particle motion, and the simulation results agree reasonably with the observed particle focusing and separation behaviors.

(Some figures in this article are in colour only in the electronic version)

1. Introduction

Dielectrophoresis (DEP) is a powerful tool that has been widely used to focus and separate cells and particles in microfluidic devices [1–3]. So far DEP has been implemented using both electrode- [4, 5] and insulator-based [6, 7] approaches to generate a non-uniform local electric field. In the former, pairs of electrodes are placed inside a microchannel, and ac voltages are applied locally through those electrodes to achieve dielectrophoretic particle deflection for either focusing [8–11] or separation [12–22]. This approach suffers from several problems such as the need of hydrodynamic pumping of the sample, the increased complexity in microchannel fabrication and the surface fouling of electrodes due to electrochemical reactions, etc [23, 24]. These problems are not encountered in the insulator-based approach, where both ac and dc fields can be applied through the electrodes positioned outside a microchannel, and the non-uniform electric field is generated by in-channel insulators.

Two types of in-channel insulators have been demonstrated to produce the dielectrophoretic force for particle and cell manipulations. The first type is the insulating obstacles (e.g. hurdles, posts and ridges) that are fabricated inside a microchannel to partially block the electric current. As a consequence, the electric field is locally amplified around the insulating obstacles, which on one hand can induce DEP for particle focusing [25, 26] or separation [27–35], while on the other hand may cause adverse effects on both the sample and the device due to Joule heating, particle clogging, etc [23]. These drawbacks are overcome in the second type of insulator-based approach where the insulating walls of a curved microchannel are directly used to control the particle motion [36]. Due to the variation in path length for electric current, the electric field becomes inherently non-uniform in a curved channel [37]. Thus, the induced dielectrophoretic force can generate a cross-stream particle deflection, which

[1] Author to whom any correspondence should be addressed.

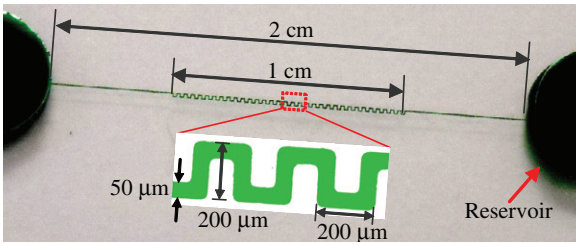

Figure 1. Picture of the serpentine microchannel used in experiments with labeled dimensions.

has been demonstrated to focus particles and cells in curved microchannels [38–40].

In our previous work, particles and cells experienced only negative DEP and were thus focused to either the centerline of a serpentine microchannel [38, 39] or the outer sidewall of a spiral microchannel [40]. This paper extends the previous work to demonstrate both the negative and positive dielectrophoretic focusing of particles in a serpentine microchannel. Moreover, these two focusing phenomena are combined to demonstrate a continuous separation between particles of different sizes and conductivities. Additionally, a numerical model is developed to simulate the observed particle focusing and separation behaviors.

2. Experiment

The serpentine microchannel was fabricated with polydimethylsiloxane (PDMS) using the standard soft lithography method. In-depth information on this procedure is referred to Church *et al* [39]. The channel consists of a straight section at each end and a serpentine section at the center; see figure 1. The serpentine section serves to focus and separate particles as explained below, and is comprised of 33 serpentine periods. The channel has a uniform width and depth, which are 50 μm and 25 μm, respectively. Polystyrene particles of 2.2 μm (fluorescent, G0220, Duke Scientific Corp.) and 5 μm (Fluka 79633, Sigma-Aldrich) in diameter were re-suspended in either deionized water or 1 mM phosphate buffer at a concentration of at least 10^7 particles per milliliter. Tween 20 (0.5% v/v, Sigma-Aldrich) was added to the suspensions to suppress particle adhesions to the channel wall as well as particle aggregations. The dc-biased ac electric field (with a fixed 1 kHz frequency) across the serpentine microchannel was supplied by a function generator (33220A, Agilent Technologies) in conjunction with a high-voltage amplifier (609E-6, Trek, Inc.). Particle motions were observed using an inverted microscope (Eclipse TE2000U, Nikon Instruments). Videos and images were recorded using a CCD camera (Nikon DS-Qi1Mc), and processed using the Nikon imaging software (NIS-ELEMENTS AR 2.30).

3. Theory

3.1. Operating mechanism

Figure 2 displays the contour of electric field intensity (the darker the higher) and the electric field lines (i.e.

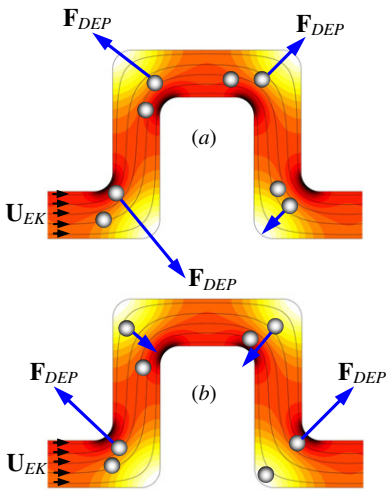

Figure 2. Mechanisms of negative (*a*) and positive (*b*) dielectrophoretic focusing of particles (shown as the shaded circles) in a serpentine microchannel. The background shows the electric field contour (the darker the higher) and the electric field lines (or equivalently the streamlines, $\mathbf{U}_{\mathrm{EK}}$) in the absence of particles. The approximate magnitude of the dielectrophoretic force, $\mathbf{F}_{\mathrm{DEP}}$, on a particle at a location is denoted by its vector length.

streamlines due to the similarity between flow and electric fields in pure electrokinetic flows [41]) in one period of the serpentine microchannel in the absence of particles. Due to the variation of electrical path, the electric field distribution at each turn becomes non-uniform generating a local maximum and minimum at the inner and outer corners, respectively. Therefore, particles experience a cross-stream dielectrophoretic force as they move electrokinetically through the channel at a velocity of $\mathbf{U}_{\mathrm{EK}}$. The time average of this force, $\mathbf{F}_{\mathrm{DEP}}$, on a spherical particle in dc and low-frequency (<100 kHz) ac electric fields is written as [42]

$$\mathbf{F}_{\mathrm{DEP}} = (1/2)\pi\varepsilon_f d^3 f_{\mathrm{CM}}(\mathbf{E}\cdot\nabla\mathbf{E}) \quad (1)$$

$$f_{\mathrm{CM}} = (\sigma_p - \sigma_f)/(\sigma_p + 2\sigma_f) \quad (2)$$

where ε_f is the permittivity of the suspending fluid, d is the particle diameter, f_{CM} is the so-called Clausius–Mossotti (CM) factor that has been assumed approximately the same in dc and low-frequency ac fields [23, 43], $\mathbf{E}$ is the root-mean-square (RMS) electric field, σ_p is the electric conductivity of the particle and σ_f is the electric conductivity of the fluid.

When the particle is less conductive than the suspending fluid, f_{CM} will be negative producing negative DEP [42, 44]. So the particle will be pushed by $\mathbf{F}_{\mathrm{DEP}}$ toward the region where the electric field is lower, i.e. the outer corners of the turns in the serpentine microchannel. In contrast, when it is more conductive than the fluid, the particle will experience positive DEP and thus be pulled by $\mathbf{F}_{\mathrm{DEP}}$ to the inner corners of the turns where the local electric field is higher. See figure 2 for the directions of $\mathbf{F}_{\mathrm{DEP}}$ on a particle in these two circumstances. As the electric field gradient is also larger at the inner corner of a turn, the particle should experience a stronger $\mathbf{F}_{\mathrm{DEP}}$ if it is closer to the inner corner. For this reason, particles undergoing negative DEP will be deflected gradually toward the channel

centerline by the alternating turns as they progress through the serpentine microchannel. This phenomenon is schematically illustrated in figure 2(*a*), where the magnitude of $\mathbf{F}_{\mathrm{DEP}}$ is denoted by its vector length. Such sheathless electrokinetic focusing in a serpentine microchannel has been recently demonstrated with both polymer particles and biological cells by the authors [38, 39].

In a similar manner, particles with positive DEP will be gradually pulled into the inner corners of the turns where the electric field strength and gradient are both stronger, and then follow the channel wall. This eventually causes a splitting with the particles lining both sidewalls of a serpentine microchannel, which is schematically illustrated in figure 2(*b*). Recognizing the distinctive focusing behaviors for particles experiencing negative and positive DEP in figure 2, one can anticipate a continuous separation between them in a serpentine microchannel. This separation mechanism was utilized to separate particles with different sizes and electric conductivities in the present work. Specifically, as suggested by equation (2), a suspending fluid with an intermediate conductivity between those of the two particles was chosen to attain simultaneously the negative and positive dielectrophoretic focusing.

3.2. Numerical modeling

In order to predict and verify the effects of negative and positive DEP on particles, a numerical model based on the Lagrangian tracking method was developed to simulate the electrokinetic particle transport through the serpentine microchannel. This model was first developed by Kang *et al* [45], where the perturbations of particles on the flow and electric fields were neglected. Instead, a correction factor, c, was introduced to account for the effects of particle size on $\mathbf{F}_{\mathrm{DEP}}$ or the resulting dielectrophoretic velocity. This model has been validated through comparisons with the experimental observations of electrokinetic particle and cell motions in various microchannels [26, 29, 35, 38–40]. In this model the particle velocity, $\mathbf{U}_p$, is expressed as [45]

$$\mathbf{U}_p = \mu_{\mathrm{EK}}\mathbf{E}_{\mathrm{DC}} + c\mu_{\mathrm{DEP}}(\mathbf{E}\cdot\nabla\mathbf{E}) + f_{p-w}(\mathbf{E}\cdot\mathbf{E})\hat{\mathbf{n}} \quad (3)$$

$$\mu_{\mathrm{DEP}} = \varepsilon_f d^2 f_{\mathrm{CM}}/6\mu_f \quad (4)$$

$$f_{p-w} = 0.176\exp[-5.734(\gamma/d)]\varepsilon_f d/3\pi\mu_f \quad (5)$$

where the three terms in equation (3) represent the particle velocities induced by electrokinetic flow, DEP and particle-wall interactions, respectively, μ_{EK} is the electrokinetic particle mobility, $\mathbf{E}_{\mathrm{DC}}$ is the dc component of the applied RMS electric field $\mathbf{E}$, μ_{DEP} is the dielectrophoretic particle mobility with μ_f being the fluid dynamic viscosity, f_{p-w} is the coefficient characterizing the wall-induced particle velocity in terms of the particle–wall separation distance γ [45] and $\hat{\mathbf{n}}$ is the unit vector normal to the channel wall. Note that the inertial and centrifugal motions have been neglected in equation (3) because the Reynolds and Dean numbers are both very small under the experimental conditions. The instantaneous position of a particle, $\mathbf{x}_p$, is then obtained by integrating the particle velocity $\mathbf{U}_p$, i.e.

$$\mathbf{x}_p = \mathbf{x}_0 + \int_0^t \mathbf{U}_p(t')\,\mathrm{d}t' \quad (6)$$

where $\mathbf{x}_0$ represents the initial location of the particle, and t is the time period from the initiation.

The numerical modeling was performed in COMSOL® (Burlington, MA) with the MATLAB® interface. A 2D model of the serpentine microchannel was first developed in COMSOL®, where the effects of the top and bottom channel walls on particle motions were ignored [26, 29, 35, 38–40]. Then, the electric field distribution that was needed to compute the particle velocity, $\mathbf{U}_p$, from equation (3) was solved from the Laplace equation in COMSOL®. Next, the finite-element-model (FEM) structure was exported into MATLAB® to determine the trajectory of a particle whose initial position was specified at the channel entrance. A custom-written program in MATLAB® was used to determine the particle position $\mathbf{x}_p$, where the key function is to calculate the particle-wall separation distance γ and thus the coefficient f_{p-w} from equation (5).

Other parameters required in the modeling were obtained as follows: the electrokinetic mobility, μ_{EK}, was attained by measuring the average particle velocity in the straight section of the serpentine microchannel; the dielectrophoretic mobility, μ_{DEP}, was determined from equation (4) using the dynamic viscosity, $\mu_f = 1.0 \times 10^{-3}$ kg m^{-1} s^{-1}, and permittivity, $\varepsilon_f = 6.9 \times 10^{-10}$ C V^{-1} m^{-1}, of pure water at 20 °C; the CM factor, f_{CM}, depends on the electric conductivities of the fluid and the particle where the latter was unable to measure and will be discussed in the next section; the correction factor, c, was determined by matching the predicted particle trajectory to the observed particle motion.

4. Results

4.1. Negative and positive dielectrophoretic particle focusing

Negative dielectrophoretic focusing in the serpentine microchannel was studied using 2.2 μm fluorescent particles suspended in a 1 mM phosphate buffer. Figure 3 shows the superimposed images (left column) at the entrance (a) and exit (b) of the channel serpentine section. The applied voltage at the inlet reservoir was 550 V ac (RMS value, 1 kHz frequency) with a 50 V dc bias while the outlet reservoir was grounded. The average electric field through the channel was about 200 V cm^{-1}. In the entrance image (figure 3(*a*)) the particles appear uniformly distributed when they enter into the serpentine section as they cover the majority of the channel width. They, however, begin to be focused in the first few serpentine periods due to the induced negative dielectrophoretic motion. At the exit of the serpentine section (figure 3(*b*)), the particles are observed to be focused to a single stream at the channel centerline with a measured width of 9 μm. This correlates well with the expected position of the particles under the influence of negative DEP, as the particles are alternately deflected away from the inner corner of each turn toward the channel centerline [38, 39].

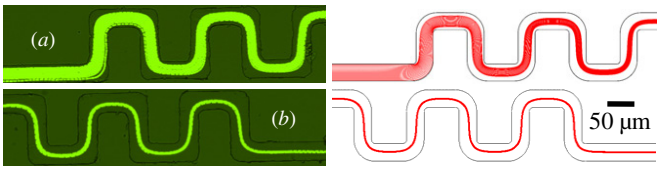

Figure 3. Superimposed images (left column) and predicted trajectories (right column) showing the negative dielectrophoretic focusing of 2.2 μm particles at the entrance (*a*) and exit (*b*) of the serpentine section of the microchannel.

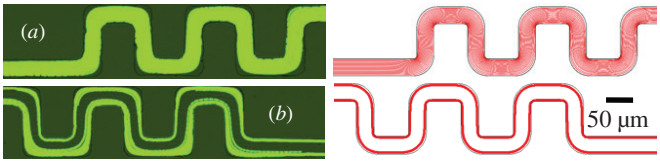

Figure 4. Superimposed images (left column) and predicted trajectories (right column) showing the positive dielectrophoretic focusing of 2.2 μm particles at the entrance (*a*) and exit (*b*) of the serpentine section of the microchannel.

The numerically predicted particle trajectories under the experimental conditions are also illustrated in figure 3 (right column) for a clear comparison. As the particle conductivity is much lower than that of 1 mM phosphate buffer (measured as 210 μS cm^{-1}) [46], the CM factor, f_{CM}, was close to -0.5 in the modeling. The particle electrokinetic mobility, μ_{EK}, was measured to be 3.0 (μm s^{-1}) (V cm^{-1})$^{-1}$. The correction factor, c, for particle DEP was set to 0.7, which was found to give a close match to the experimental results.

Positive dielectrophoretic focusing in the serpentine microchannel was tested using the same 2.2 μm particles as in the negative DEP experiment. In order to ensure positive DEP, deionized water was used as the suspending fluid due to its extremely low electric conductivity. Figure 4 (left column) shows the superimposed images at the entrance (a) and exit (b) of the channel serpentine section. The same electric field as used in the negative DEP experiment was applied. At the entrance region (figure 4(*a*)), the particles once again appear scattered and uniformly distributed covering the majority of the channel width. However, from the exit image in figure 4(*b*), the particles can be observed lining the sidewalls of the channel with a measured width of about 9 μm on each side. This is also consistent with the theory as the particles should be attracted by positive DEP to the high electric field region at the inner corner of the channel turns.

The numerically predicted particle trajectories for positive dielectrophoretic focusing in the serpentine microchannel are illustrated in the right column of figure 4. For the modeling, the average electrokinetic mobility, μ_{EK}, of 2.2 μm particles in deionized water was measured to be 3.5 (μm s^{-1}) (V cm^{-1})$^{-1}$. The CM factor, f_{CM}, was assumed to be +0.2 while the correction factor, c, was set to 0.4. The CM factor was obtained by assuming that (1) the electric conductivity of 2.2 μm particles is about 9 μS cm^{-1}, equivalent to a 0.5 nS surface conductance [46], and (2) the electric conductivity of the deionized water is around 5 μS cm^{-1} which could not be measured accurately due to the limitation of the conductivity meter (accumet AP85, Fisher Scientific, unable to be calibrated below 12 μS cm^{-1}). The correction factor used here is significantly smaller than that used in modeling the negative dielectrophoretic focusing of the same particle (which is 0.7). The reason behind this discrepancy is currently unknown. With these parameters, the modeling results seem to predict the experimental observations reasonably well.

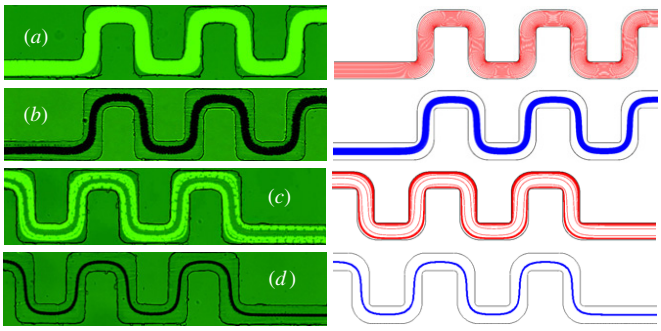

Figure 5. Superimposed images (left column) and predicted trajectories (right column) showing the separation of 2.2 μm fluorescent particles and 5 μm non-fluorescent particles in the serpentine microchannel: (*a*) 2.2 μm particles at the entrance, (*b*) 5 μm particles at the entrance, (*c*) 2.2 μm particles at the exit and (*d*) 5 μm particles at the exit of the serpentine section.

4.2. Particle separation via negative and positive dielectrophoretic focusing

The negative and positive dielectrophoretic focusing phenomena as demonstrated above were combined to achieve particle separation in the serpentine microchannel. For this experiment, 2.2 μm and 5 μm particles were mixed and suspended in deionized water. The calculated electric conductivity of 5 μm particles was about 4 μS cm^{-1} if the surface conductance was still assumed to be 0.5 nS [46]. Thus, the CM factor for 5 μm particles in deionized water (with the electric conductivity being still assumed as 5 μS cm^{-1}) was approximately -0.07, yielding negative DEP. Therefore, 5 μm and 2.2 μm particles should be focused to the centerline and the sidewalls of the serpentine microchannel, respectively, and can thus be continuously separated without any other external force. Figure 5 (left column) shows the superimposed images of particle separation at the entrance ((a) for 2.2 μm particles and (b) for 5 μm particles) and exit ((c) for 2.2 μm particles and (d) for 5 μm particles) of the channel serpentine section. The applied voltage was 500 V ac (RMS value, 1 kHz frequency) with a 100 V dc bias. Note that the superimposed images for the two types of particles are from the same video though they are displayed individually.

In the entrance region of the serpentine section, both the fluorescent 2.2 μm particles (figure 5(*a*)) and the non-fluorescent 5 μm particles (figure 5(*b*)) are unfocused and (nearly) uniformly distributed. At the exit region, the two different dielectrophoretic focusing behaviors can be seen clearly. As expected 2.2 μm particles are observed in figure 5(*c*) to line the channel sidewalls due to positive DEP while 5 μm particles are focused by negative DEP

to the channel centerline in figure 5(*d*). However, the positive dielectrophoretic focusing of 2.2 μm particles (with a measured stream width of about 15 μm on either sidewall) appears to be less effective than the negative dielectrophoretic focusing of 5 μm particles (with a measured stream width of about 8 μm). This is mainly attributed to the strong dependence of dielectrophoretic force on a particle size, see equation (1). In addition, the focusing of 2.2 μm particles is weaker than that in figure 4 because the particles spend less time in the channel to experience the dielectrophoretic force in a larger dc field. At this point, if a three-fork branch could be included slightly downstream of the serpentine section, the 2.2 μm fluorescent particles would be filtered outward through the side branches while the 5 μm particles continued forward along the center branch.

The numerically predicted trajectories for 2.2 μm and 5 μm particles in the separation experiment are displayed in the right column of figure 5. In the modeling the electrokinetic mobility, μ_{EK}, of 2.2 μm particles in deionized water was as given earlier while that of 5 μm particles was measured to be 5.5 (μm s^{-1}) (V cm^{-1})$^{-1}$. The CM factor of 2.2 μm particles was still assumed to be +0.2 with the same correction factor as in the positive dielectrophoretic focusing experiment, i.e. $c = 0.4$. For 5 μm particles, the CM factor was -0.07 as discussed above, and the correction factor was set to 0.5 which is consistent with the previous studies [26, 38–40]. With these parameters, the modeling results agree with the experimental observations reasonably well.

5. Conclusions

Negative and positive dielectrophoretic focusing of particles have been both demonstrated in a serpentine microchannel by changing the electric conductivity of the suspending fluid. Particles were observed to either move along the channel centerline or line the channel sidewalls when their electric conductivity was lower (yielding negative DEP) or higher (yielding positive DEP) than that of the fluid. In both cases focusing takes place due to the cross-stream migration of particles caused by the dielectrophoretic force induced by the channel turns. As particles are focused to different regions of the serpentine microchannel with negative and positive DEP, the two phenomena have also been combined to demonstrate a continuous separation between particles of different sizes. In this separation the more conductive smaller particles experienced positive DEP and were focused to the channel sidewalls, while the less conductive larger particles experienced negative DEP and were thus focused to the channel centerline. A numerical model based on the Lagrangian tracking method has also been developed, which can predict reasonably the observed particle focusing and separation behaviors in the serpentine microchannel.

Acknowledgments

This work was supported by NSF under grant CBET-0853873 with Marc S Ingber as the grant monitor. The support from Clemson University through the Creative Inquiry Program is also gratefully acknowledged.

References

[1] Pamme N 2007 *Lab Chip* **7** 1644–59
[2] Kersaudy-Kerhoas M, Dhariwal R and Desmulliez M P Y 2008 *IET Nanobiotechnol.* **2** 1–13
[3] Tsutsui H and Ho C M 2009 *Mech. Res. Commun.* **36** 92–103
[4] Hughes M P 2002 *Electrophoresis* **23** 2569–82
[5] Gascoyne P R C and Vykoukal J V 2004 *Proc. IEEE* **92** 22–42
[6] Lapizco-Encinas B H and Rito-Palmomares M 2007 *Electrophoresis* **28** 4521–38
[7] Chou C F and Zenhausern F 2003 *IEEE Eng. Med. Biol. Mag.* **22** 62–7
[8] Lin C H, Lee G B, Fu L M and Hwey B H 2004 *J. Microelectromech. Syst.* **13** 923–32
[9] Yu C, Vykoukal J, Vykoukal D M, Schwartz J A, Shi L and Gascoyne P R C 2005 *J. Microelectromech. Syst.* **14** 480–7
[10] Holmes D, Morgan H and Green N G 2006 *Biosens. Bioelectron.* **21** 1621–30
[11] Cheng I F, Chang H C, Hou D and Chang H C 2007 *Biomicrofluidics* **1** 021503
[12] Choi S and Park J K 2005 *Lab Chip* **5** 1161–7
[13] Hu X, Bessette P H, Qian J R, Meinhart C D, Daugherty P S and Soh H T 2005 *Proc. Natl Acad. Sci.* **102** 15757–61
[14] James C D, Okandan M, Mani S S, Galambos P C and Shul R 2006 *J. Micromech. Microeng.* **16** 1909–18
[15] Kralj J G, Lis M T W, Schmidt M A and Jensen K F 2006 *Anal. Chem.* **78** 5019–25
[16] Li Y, Dalton C, Crabtree H J, Nilsson G and Kaler K V I S 2007 *Lab Chip* **7** 239–48
[17] Braschler T, Demierre N, Nascimento E and Silva T 2008 *Lab Chip* **8** 280–6
[18] Han K H and Razier A B 2008 *Lab Chip* **8** 1079–86
[19] Chang S and Cho Y 2008 *Lab Chip* **8** 1930–6
[20] Song H, Mulukutla V, James C D and Bennett D J 2008 *J. Micromech. Microeng.* **18** 125013
[21] Wang L, Lu J, Marchenko S A, Monuki E S, Flanagan L A and Lee A P 2009 *Electrophoresis* **30** 782–91
[22] Khoshmanesh K, Zhang C, Tovar-Lopez F J, Nahavandi S, Baratachi S, Kalantar-Zadeh K and Mitchell A 2009 *Electrophoresis* **30** 3707–17
[23] Voldman J 2006 *Annu. Rev. Biomed. Eng.* **8** 425–54
[24] Lin R, Ho C, Liu C and Chang H 2006 *Biotechnol. J.* **1** 949–57
[25] Thwar P K, Linderman J J and Burns M A 2007 *Electrophoresis* **28** 4572–81
[26] Zhu J and Xuan X 2009 *Electrophoresis* **30** 2668–75
[27] Lapizco-Encinas B H, Simmons B A, Cummings E B and Fintschenko Y 2004 *Anal. Chem.* **76** 1571–9
[28] Lapizco-Encinas B H, Simmons B A, Cummings E B and Fintschenko Y 2004 *Electrophoresis* **25** 1695–704
[29] Kang K, Kang Y, Xuan X and Li D 2006 *Electrophoresis* **27** 694–702
[30] Pysher M D and Hayes M A 2007 *Anal. Chem.* **79** 4552–7
[31] Ozuna-Chacón S, Lapizco-Encinas B H, Rito-Palomares M, Martínez-Chapa S O and Reyes-Betanzo C 2008 *Electrophoresis* **29** 3115–22
[32] Hawkins B G, Smith A E, Syed Y A and Kirby B J 2007 *Anal. Chem.* **79** 7291–300
[33] Kang Y, Li D, Kalams S A and Eid J E 2008 *Biomed. Microdev.* **10** 243–9
[34] Lewpiriyawong N, Yang C and Lam Y C 2008 *Biomicrofluidics* **2** 034105
[35] Kang Y, Cetin B, Wu Z and Li D 2009 *Electrochim. Acta* **54** 1715–20

[36] Ai Y, Park S, Zhu J, Xuan X, Beskok A and Qian S 2010 *Langmuir* **26** 2937–44
[37] Davison S M and Sharp K V 2008 *Microfluid. Nanofluid.* **4** 409–18
[38] Zhu J, Tzeng T J, Hu G and Xuan X 2009 *Microfluid. Nanofluid.* **7** 751–6
[39] Church C, Zhu J, Wang G, Tzeng T J and Xuan X 2009 *Biomicrofluidics* **3** 044109
[40] Zhu J and Xuan X 2009 *J. Colloid Interface Sci.* **340** 285–90
[41] Cummings E B, Griffiths S K, Nilson R H and Paul P H 2000 *Anal. Chem.* **72** 2526–32
[42] Morgan H and Green N G 2002 *AC Electrokinetic: Colloids and Nanoparticles* (Baldock: Research Studies Press)
[43] Cummings E B and Singh A K 2003 *Anal. Chem.* **75** 4724–31
[44] Pohl H A 1978 *Dielectrophoresis* (Cambridge: Cambridge University Press)
[45] Kang K, Xuan X, Kang Y and Li D 2006 *J. Appl. Phys.* **99** 064702
[46] Ermolina I and Morgan H 2005 *J. Colloid Interface Sci.* **285** 419–28